Influence of pH on ZnO nanocrystalline thin films prepared by sol–gel dip coating method

K SIVAKUMAR[a,b], **V SENTHIL KUMAR**[a], **N MUTHUKUMARASAMY**[c], **M THAMBIDURAI**[c,*] **and T S SENTHIL**[d]

[a]Department of Physics, Karpagam University, Coimbatore 641 021, India
[b]Department of Physics, Hindusthan College of Engineering and Technology, Coimbatore 641 032, India
[c]Department of Physics, Coimbatore Institute of Technology, Coimbatore 641 014, India
[d]Department of Physics, Erode Sengunthar Engineering College, Erode 638 057, India

Abstract. ZnO nanocrystalline thin films have been prepared on glass substrates by sol–gel dip coating method. ZnO thin films have been coated at room temperature and at four different pH values of 4, 6, 8 and 10. The X-ray diffraction pattern showed that ZnO nanocrystalline thin films are of hexagonal structure and the grain size was found to be in the range of 25–45 nm. Scanning electron microscopic images show that the surface morphology improves with increase of pH values. TEM analysis reveals formation of ZnO nanocrystalline with an average grain size of 44 nm. The compositional analysis results show that Zn and O are present in the sample. Optical band studies show that the films are highly transparent and exhibit a direct bandgap. The bandgap has been found to lie in the range of 3·14–3·32 eV depending on pH suggesting the formation of ZnO nanocrystalline thin films.

Keywords. Sol–gel; ZnO nanocrystalline thin films; dip coating method.

1. Introduction

ZnO materials have attracted much interest due to wide direct bandgap of 3·37 eV and large exciton binding energy of 60 meV. Semiconductor nanoparticles have attracted much attention in recent years due to novel optical, electrical and mechanical properties, which results from quantum confinement effects compared with their bulk counterparts. Among various semiconductor nanoparticles, nano-sized zinc oxide (ZnO) particles are the most frequently studied because of their interest in fundamental study and also their applied aspects such as in dye sensitized solar cell (Wu *et al* 2007), gas sensors (Chen *et al* 2011), microwave absorber (Zhou *et al* 1999), optical switches (Kind *et al* 2002) and light emitting diodes (Kim *et al* 2002). ZnO semiconductor has several favourable properties such as good transparency, high electron mobility, wide bandgap and strong room-temperature luminescence. ZnO thin films have been prepared by different researchers using various techniques such as physical vapour deposition (Kouam *et al* 2008), chemical vapour deposition (Wang *et al* 2011), sputtering (Zhang *et al* 2010), spray pyrolysis (Ayouchi *et al* 2003), and sol–gel method (Yakuphanoglu *et al* 2010). The sol–gel technique is extensively studied as a matrix material method to produce nanocomposites because it gives a higher specific surface area, superior homogeneity and purity, better microstructural control of metallic particles, narrow pore size and uniform particle distribution. In addition, the sol–gel method also offers several other advantages, like low temperature processing, possibility of coating on large area substrates and most importantly it is cost effective. In the present study, ZnO thin films have been prepared using zinc acetate dihydrate and 2-methoxy ethanol by the simple sol–gel dip coating method at room temperature. An attempt has been made to control the hydrolysis/condensation reaction in the sol–gel of ZnO using mono ethanolamine. The effect of preparative parameter, pH, of the sol on the properties of the prepared ZnO films has been studied.

2. Experimental

Zinc acetate dihydrate was used as zinc precursor; the matrix sol was prepared by mixing zinc acetate dihydrate with absolute 2-ethoxyethanol and monoethanolamine at room temperature. 2-methoxy ethanol and monoethanolamine were used as solvent and stabilizing agent, respectively. Monoethanolamine was used to control pH of condensation reaction in sol–gel solution. The molar ratio of MEA to zinc acetate was kept at 1·0 and the concentration of zinc acetate was 0·75 m. The resultant solution was stirred at 60°C for 30 min to yield a clear and homogeneous solution, and this solution was used as coating solution. ZnO film was formed by dipping well cleaned glass substrates into the sol at room temperature. Film deposition was carried out in air at room temperature by the dip coating method with a controlled withdrawal speed of 2 cm min^{-1}. The film was

*Author for correspondence (phy_thambi@rediffmail.com)

heated at 100°C for 10 min and then allowed to cool to room temperature. ZnO was again dip coated on the already coated ZnO film and heated at 100°C for 10 min and then allowed to cool up to room temperature. The dip coating, heating and cooling process was repeated four times in order to get thicker films. The film was then dried at room temperature for 2 h and then annealed in air at 500°C for 1 h using a heating rate of 2°C/min.

X-ray diffraction studies have been carried out using PANalytical X-ray diffractometer. Surface morphology of the samples was studied using scanning electron microscope (JEOL JSMS 800-V). Transmission electron microscopic (TEM) images of the prepared ZnO were recorded using a Philips TECNAI F20 microscope. Compositional analysis of the samples was studied using energy dispersive analysis of X-rays (JEOL Model JED -2300). Optical characterization of the films was carried out using UV–VIS–NIR spectrophotometer (Jasco V-570).

3. Results and discussion

Figure 1 shows X-ray diffraction pattern of ZnO thin films prepared at four different pH values of 4, 6, 8 and 10. The diffraction pattern shows small peaks revealing that the prepared films are made of small crystallites. Peaks corresponding to the (100), (002), (101), (102), (110) and (103) planes of hexagonal ZnO is observed. The diffraction pattern exhibits all the characteristic peaks of the wurtzite ZnO hexagonal $P6(3)mc$ structure, according to JCPDS card file No. 36-1451. No other peaks are observed, suggesting that only single-phase ZnO has formed. ZnO nanostructured samples grown for various pH values have the same hexagonal wurtzite structure, with no indication of impurities. The growth rate of the film has been found to decrease with pH. It shows a higher growth rate at a pH around 4 and a lower growth rate at about pH 10. For the pH values below
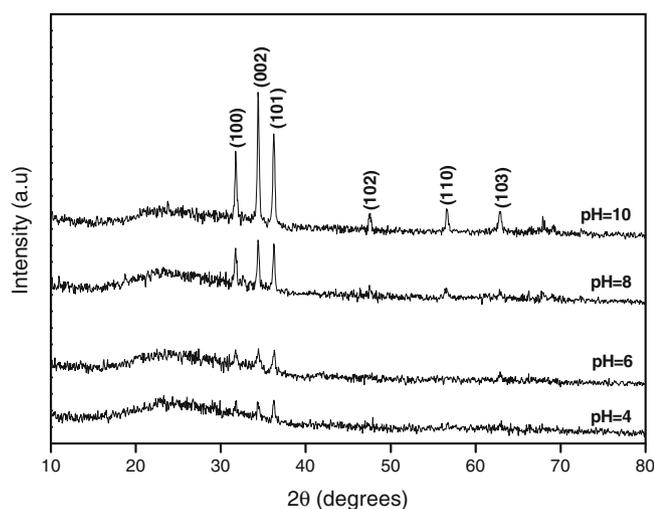
4, the deposition rate was very fast, but the film did not adhere to the substrate, formed as aggregates on the surface, and peeled off from the substrate in the solution itself. The electrolyte bath solution with a pH in the range 4–10 was found to result in smooth films with good adherence. Addition of monoethanolamine to zinc acetate solution transforms the nature of the sol from acidic to alkaline by changing the pH value from 4 to 10. The investigations indicate that high quality ZnO films are obtained by using sol having monoethanolamine to zinc acetate ratio of 1:1. The intensity of the peaks in the diffraction pattern is found to increase with increase in pH value. This suggests that increase in pH helps in nucleation and growth of grains. Low pH value corresponds to acidic solution and this generally could restrain grain growth. When the pH value is beyond 6 a total alkali environment prevails and this enhances grain growth. Acidic solution restrains hydrolysis while alkali can accelerate hydrolysis during reaction. When pH is beyond 6 the environment is favourable to accelerate hydrolysis and large aggregated particles are formed and grain tends to grow quickly. The lattice parameter values, a and c, have been calculated and are 3·24 Å and 5·21 Å, respectively and are in good agreement with the reported standard values (JCPDS No. 36-1451). The average grain size has been calculated using Scherrer formula (Maleki 2007):

$$D = 0·94\lambda/\beta \cos\theta, \tag{1}$$

where D is the mean crystallite size, β the full width at half maximum of the diffraction line, θ the angle of diffraction, and λ the wavelength of the X-ray radiation. The crystallite size obtained was 23, 27, 32 and 45 for pH of 4, 6, 8 and 10, respectively. From these values it is observed that the particle size increases with increase in pH value.

The first principle study shows that the Zn_{3d} electrons strongly interact with the O_{2p} electron in ZnO (Vanheusden 1996). Oxygen has tightly bound $2p$ electron and Zn has tightly bound $3d$ electron which sense the nuclear attraction efficiently. The rate of hydrolysis decreases with increasing pH. In the initial growth stage, the pH and the concentration of Zn^{2+} ions is such that the ZnO growth will be through $Zn(OH)_2$. With the gradual increase of pH and the decrease in the concentration of Zn ions, $Zn(OH)_2$ becomes thermodynamically unstable and the $Zn(OH)_2$ formed on the substrate will start dissolving. Further growth of nanostructure will have been through direct deposition of ZnO. The pH affects the hydrolysis and condensation behaviour of the solution during gel formation and therefore, influences the morphology of ZnO (Wahab *et al* 2009). The basic nature of the modified sol as a function of increase in the ratio of additive MEA to ZnAc precursor (R) was investigated. The increase in pH with addition of MEA clearly indicates an increase of alkaline nature of the prepared sols. This increase is attributed to hydrolysis of salts of weak acid in strong base medium. The higher alkaline nature of sols is reported to be useful in enhancing the formation of ZnO crystallites (Znaidi *et al* 2003).
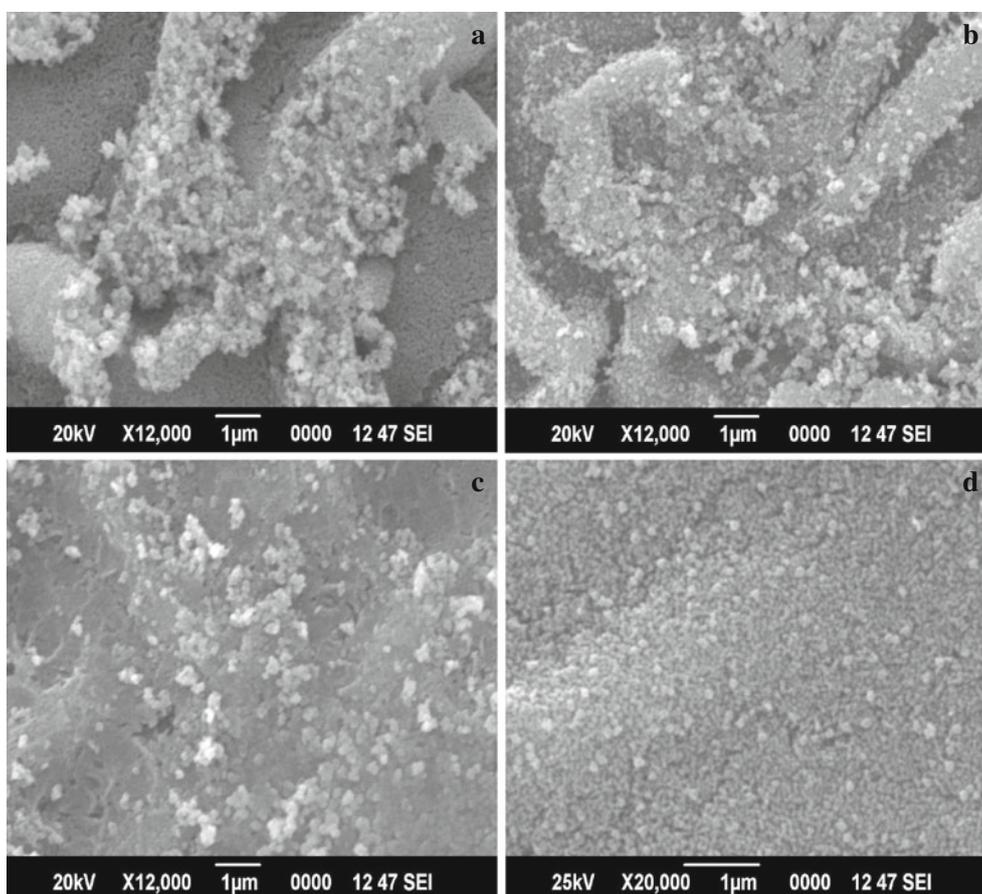

Figure 1. X-ray diffraction pattern of ZnO nanocrystalline thin films.

Figure 2. SEM micrographs of ZnO thin films deposited using different pH values (**a**) pH = 4, (**b**) pH = 6, (**c**) pH = 8 and (**d**) pH = 10.

Scanning electron microscope images of ZnO films deposited at different pH values are shown in figures 2(a)–(d). A strong influence of pH on the crystalline growth is clearly observed from the micrograph. The surface morphology of the films is found to improve with increase in increasing pH values. The size distribution of grains appears to be less homogenous for lower pH values. SEM images show distinguished spherical morphology with self-aligned prismatic nanoparticles. The morphology of particles is to be found roughly spherical and homogenous; some of the particles have agglomerated. Figure 3 shows transmission electron microscope (TEM) image of prepared ZnO nanocrystalline thin film for pH of 10. TEM image gives a grain size of 44 nm and this is in agreement with X-ray diffraction result. The diffraction pattern illustrating spot patterns of the hexagonal structure of ZnO indicates that the ZnO nanoparticles formed using a pH are highly crystalline, which is in good agreement with the X-ray diffraction result. Figure 4 shows energy dispersive analysis of X-ray spectra of ZnO and results show that 49·65 % Zn and 50·35 % of O are present in the sample.

Figure 5 shows optical transmittance spectra of ZnO films prepared at different pH values. The transmittance for the film prepared at lower pH value was observed to be the
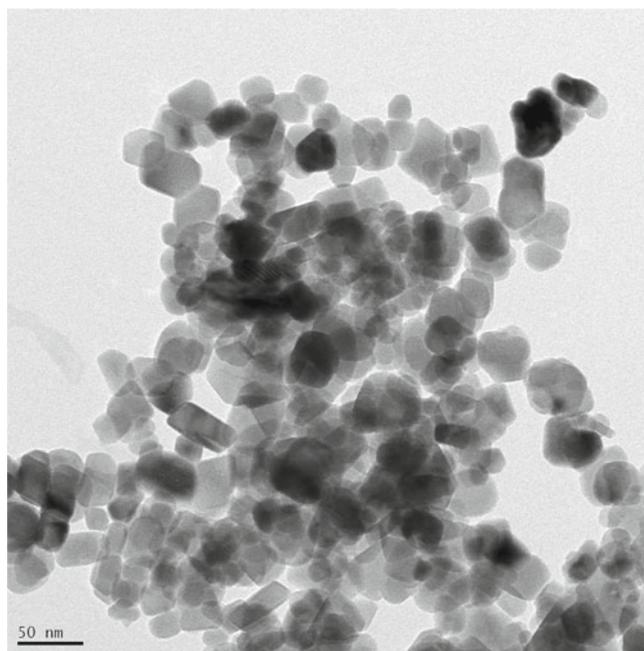

Figure 3. TEM image of ZnO nanocrystalline thin film for pH of 10.

highest ($\sim 85\%$ at 900 nm). The transmittance of the film is observed to decrease with increase in pH value. This can be ascribed to the formation of larger particles on the surface of ZnO thin films with increase of pH value which causes scattering of light. The absorption coefficient (α) of the deposited ZnO films has been found to be of the order of 10^4 cm^{-1}. The study of the absorption coefficient in the fundamental region and near the fundamental edge provides valuable information about the energy band structure of the material. The nature of transition and bandgap of the ZnO thin films have been determined by plotting $(\alpha h\nu)^p$ against the photon energy, $h\nu$. The plots $(\alpha h\nu)^{2/3}$ vs $h\nu$ (direct forbidden), $(\alpha h\nu)^{1/2}$ vs $h\nu$ (indirect allowed), $(\alpha h\nu)^{1/3}$ vs $h\nu$ (indirect forbidden) of ZnO thin films did not exhibit straight line over any part of the optical spectrum, thus supporting that the type of transition in ZnO thin films is neither direct forbidden nor indirect. Plot of $(\alpha h\nu)^2$ vs $h\nu$ of the deposited ZnO films are shown in figure 6. The straight line nature of the plots shows that the transition in the prepared ZnO films is direct allowed and the bandgap is found to be 3·32 eV, 3·24 eV, 3·19 eV and 3·14e V for the pH values of 4, 6, 8 and 10, respectively. The grain size increases with increase in pH of the precursor solution. The bandgap decreases with increase in pH due to the increase of grain size (Houng *et al* 2007). This decrease in
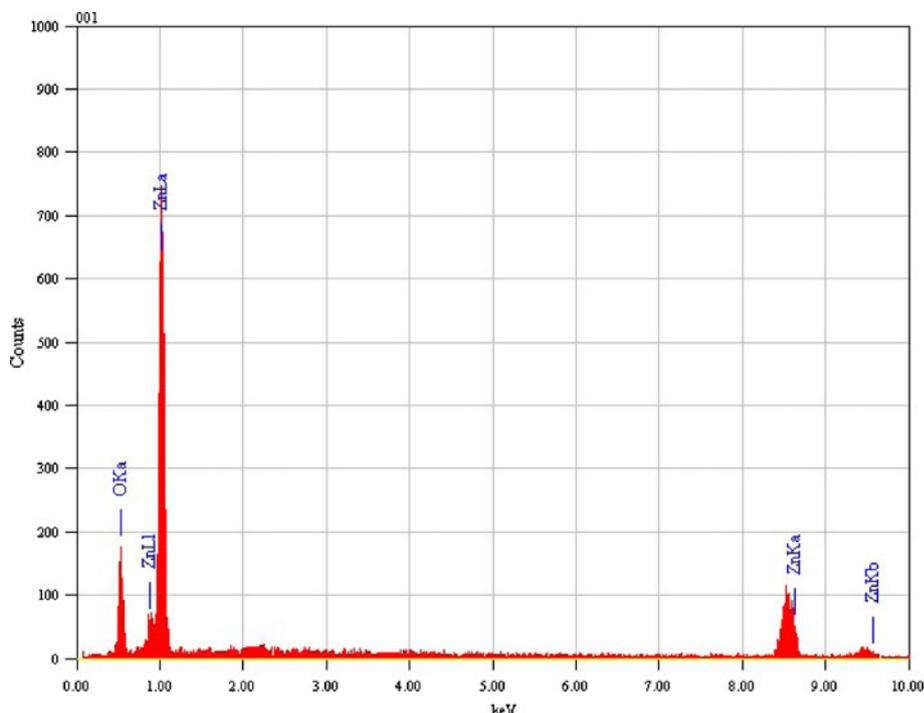

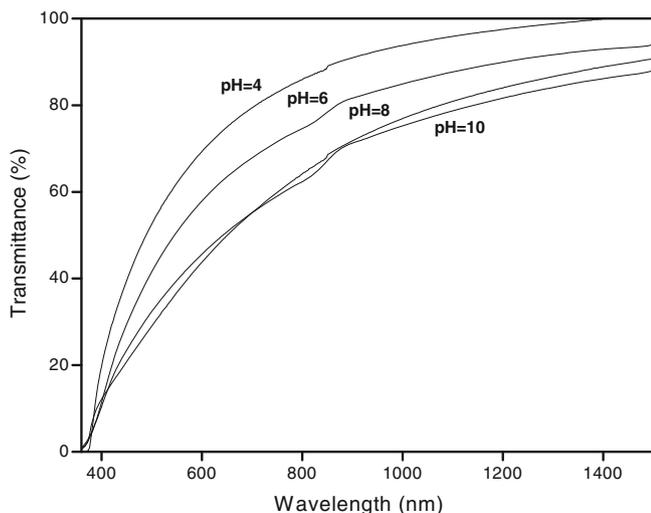**Figure 4.** EDAX spectra of ZnO thin film for pH of 10.

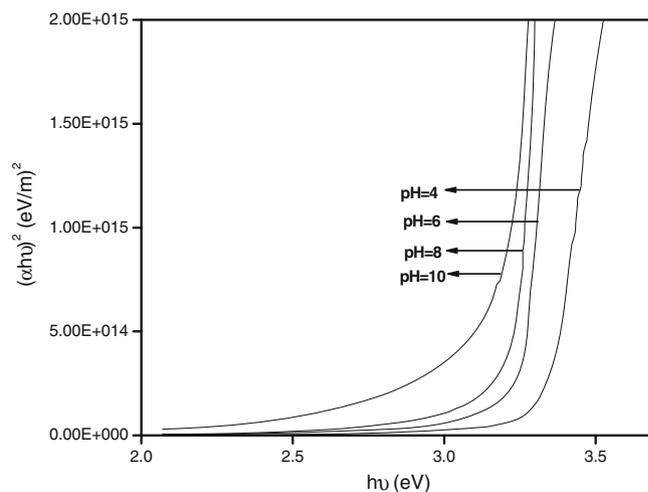**Figure 5.** Transmittance spectra of ZnO nanocrystalline films.

Figure 6. Plot of $(\alpha h\nu)^2$ vs $h\nu$ of ZnO nanocrystalline thin films.

bandgap causes a strong red shift in the optical spectra, due to agglomeration of the nanocrystallites into larger crystallites.

4. Conclusions

ZnO nanocrystalline thin films have been prepared on glass substrate by sol–gel dip coating method. X-ray diffraction analysis reveals that ZnO is in hexagonal structure. Scanning electron microscopic images show that the grain size increases with increase in pH. The compositional analysis results show that Zn and O are present in the sample. The increase in pH values of range 4, 6, 8 and 10 decreases the bandgap energy from 3·32 to 3·14 eV.

References

Ayouchi R, Leinen D, Martín F, Gabas M, Dalchiele E and Ramos-Barrado J R 2003 *Thin Solid Films* **426** 68

Chen Jin, Li Jin, Li Jiahui, Xiao Guoqing and Yang Xiaofeng 2011 *J. Alloys Compd.* **509** 740

Houng Boen, Huang Cheng-Lou and Tsa Song-Yuan 2007 *J. Cryst. Growth* **307** 328

Kim K, Horwitz J S, Kim W H, Makinen A J, Kafafi Z H and Chrisey D B 2002 *Thin Solid Films* **420–421** 539

Kind H, Yan H Q, Messer B, Law M and Yang P D 2002 *Adv. Mater.* **14** 158

Kouam J, Ait-Ahcene T, Plaiasu A G, Abrudeanu M, Motoc A, Beche E and Monty C 2008 *Solar Energy* **82** 226

Maleki M, Ghamsari M Sasani, Mirdamadi Sh. and Ghasemzadeh R 2007 *Semicond. Phys. Quant. Electron. Optoelectron.* **10** 30

Vanheusden K, Warren W L, Seager C H, Tallant D R, Voigt J A and Gnade B E 1996 *J. Appl. Phys.* **79** 7983

Wahab R, Ansari S G, Kim Y S, Song M and Shin H S 2009 *Appl. Surf. Sci.* **255** 4891

Wang X H, Li R B and Fan D H 2011 *Appl. Surf. Sci.* **257** 2960

Wu Jih-Jen, Chen Guan-Ren, Yang Hung-Hsien, Ku Chen-Hao and La Jr-Yuan 2007 *Appl. Phys. Lett.* **90** 213109

Yakuphanoglu Fahrettin 2010 *J. Alloys Compd.* **507** 184

Zhang Zhonghai, Hossain Md Faruk, Arakawa Takuya and Takahashi Takakazu 2010 *J. Hazard. Mater.* **176** 973

Zhou Z W, Peng W M, Ke S Y and Deng H 1999 *J. Mater. Proc. Technol.* **89–90** 415

Znaidi L, Solar Illa G J A A, Benyahia S and Kanaev A V 2003 *Thin Solid Films* **482** 257